Project 066 Evaluation of High-Thermal-Stability Fuels

Washington State University

Project Lead Investigator

Joshua Heyne
Bioproducts, Sciences, and Engineering Laboratory Director, Associate Professor
School of Engineering and Applied Science
Washington State University
2710 Crimson Way, Richland, WA 99354
(937) 229-5319
joshua.heyne@wsu.edu

University Participants

Washington State University (WSU)

- P.I.s: Assoc. Prof. Joshua Heyne and Assoc. Res. Prof. Randall Boehm
- FAA Award Number: 13-C-AJFE-WaSU-036
- Period of Performance: October 1, 2024, to September 30, 2025
- Tasks:
  1. Perform Jet Fuel Oxidation Tester (JFTOT) repeatability and reproducibility assessment
  2. Gain proficiency in analytical methods for trace impurities detection
  3. Develop methods for natural impurities amplification
  4. Establish a detailed experimental test plan for evaluating thermal stability
  5. Execute thermal stability test campaign

Project Funding Level

The Federal Aviation Administration (FAA) provided $350,000 in funding. Cost-sharing funding is provided by Air Company Holdings, Inc. ($350,000).

Investigation Team

Washington State University

Assoc. Prof. Joshua Heyne, (P.I.), All Tasks
Assoc. Res. Prof. Randall Boehm, (co-P.I.), All Tasks
Conor Faulhaber, (graduate research student), All Tasks

Project Overview

It has long been understood that increasing the reliance on jet fuel as a primary coolant for both the engine and the aircraft has significant performance and efficiency benefits relative to the use of air as a coolant (Bruening & Chang, 1999), but fuel degradation and coking at high temperatures restrict how much heat can be put into the fuel. In some military applications, the performance benefits are sufficiently large to justify the creation of specialty fuels such as JP7 and Jet Propellant Thermally Stable (JPTS), which can tolerate much higher temperatures than petroleum-derived Jet A or Jet A1 (JP8) fuels (Edwards, 2007). In land-based applications of gas turbines, weight is of little consequence; thus, the operations of waste heat recovery (WHR) for plant efficiency or the cooling of combustor inlet temperature for emission reductions can be accomplished in a wide variety of ways, all of which are impractical for flight because of their impact on the mass of the power plant. Nonetheless, these applications provide some common examples of how controlling the air temperature along its flow path through the engine can have a large impact on performance, durability, and energy efficiency (Wilfert et al., 2007). The flurry of works relating to fuel deoxygenation (Zabarnick et al., 2020) and other ways to decrease coking propensity and its impacts (Mancini et al., 2004) is largely motived at the sponsorship level by these benefits.

More recently, sustainable aviation fuels (SAF) have received much attention because they can contribute to high-priority geopolitical goals to diversify energy supply chains and reduce greenhouse gas emissions. Most of these efforts have focused on streamlining the evaluation and approval processes to use synthetic fuels at some blend ratio with petroleum-derived jet fuel to create a so-called drop-in fuel that can be used within existing infrastructure without objection from any stakeholders (Colket & Heyne, 2021). Additionally, there have been discussions regarding characteristics of synthetic blend components (e.g., low aromatics, high specific energy, and high thermal stability) that would make these components attractive to consider as potential specialty fuels (i.e., JPTS) or high-performance fuels. Kosir et al. (2020) published work highlighting the efficiency gain that could be realized by using fuels with high specific energy, via lower aircraft weight at take-off, with less mass to lift and hold against the force of gravity.

The weight of fuel uplifted to an aircraft, as necessary to complete its mission, is certainly an important component to consider in assessing the integrated engine/aircraft energy demand and efficiency. The energy efficiency of the engine is also expected to be influenced by other fuel properties, including the following:

- **Hydrogen/carbon (H/C) ratio:** Through its impact on combustor exhaust gas composition, this ratio has a small impact on the ratio of heat capacities (gamma), combustor exit temperature, and work extracted during expansion through the turbine, even when the total enthalpy created at the combustor is unchanged.
- **Viscosity:** Viscosity impacts the heat transfer coefficients, which determine how much waste heat is recovered by the fuel (coolant) and delivered back to the engine via the combustor.
- **Energy density:** Energy density, measured in joules per liter (J/L), impacts volumetric flow rates, which also impacts heat transfer coefficients.
- **Specific heat:** Specific heat also has some effect on heat transfer coefficients, but perhaps more importantly has a direct impact on the temperature rise in the fuel per unit of heat energy absorbed, which in turn may impact the coking rate.
- **Coking rate:** Also known as fuel thermal stability, the coking rate drives several high-level design decisions relating to the thermal management of an engine.

References

Bruening, G. B., & Chang, W. S. (1999). Cooled cooling air systems for turbine thermal management. *Proceedings of the ASME 1999 International Gas Turbine and Aeroengine Congress and Exhibition. Volume 3: Heat Transfer; Electric Power; Industrial and Cogeneration*, Indianapolis, Indiana. https://doi.org/10.1115/99-GT-014

Colket, M., & Heyne, J. (2021). *Fuel effects on operability of aircraft gas turbine combustors*. The American Institute of Aeronautics and Astronautics, Inc. https://doi.org/10.2514/4.106040

Edwards, T. (2007). Advancements in gas turbine fuels from 1943 to 2005. *Journal of Engineering for Gas Turbines and Power, 129*(1), 13–20. https://doi.org/10.1115/1.2364007

Kosir, S., Stachler, R., Heyne, J., & Hauck, F. (2020). High-performance jet fuel optimization and uncertainty analysis. *Fuel, 281*. https://doi.org/10.1016/j.fuel.2020.118718

Mancini, A. A., Ackerman, J. F., Richard, L. K., & Stowell, W. R. (2004). *Method and coating system for reducing carbonaceous deposits on surfaces exposed to hydrocarbon fuels at elevated temperatures* (6808816 B2). General Electric Company.

Wilfert, G., Sieber, J., Rolt, A., Baker, N., Touyeras, A., & Colantuoni, S. (2007). *New environmental friendly aero engine core concepts*. https://api.semanticscholar.org/CorpusID:73527508

Zabarnick, S., West, Z. J., Arts, A., Griesenbrock, M., & Wrzesinski, P. (2020). Studies of the impact of fuel deoxygenation on the formation of autoxidative deposits. *Energy Fuels, 34*, 13814–13821. https://doi.org/10.1021/acs.energyfuels.0c02603

Task 1 – Perform Jet Fuel Thermal Oxidation Tester Repeatability and Reproducibility Assessment

Washington State University

Objective

The objective of Task 1 is to establish the repeatability and reproducibility of the JFTOT measurement. Doing so will provide a foundation for determining the thermal stability impacts of varying SAF impurity profiles, begin to evaluate the effectiveness of the current specification's trace impurity limits on reducing thermal stability risks for novel SAF, and explore the potential of improved thermal stability relative to conventional fuels.

Research Approach

The repeatability assessment was accomplished by performing 22 total JFTOT measurements over seven temperature settings on a conventional Jet A fuel ("Richland Jet A") sourced from a local airport. Other than varying temperature, tests were run under conditions abiding by the standard ASTM D3241 specifications (ASTM, 2023b) on Falex® 400 JFTOT. The JFTOT sample tubes (aluminum, Falex, Inc.) were rated for total deposit thickness using the ellipsometric method described in ASTM D3241 Annex 3 on a Falex 430 ellipsometric tube rater (ETR). The repeatability was also evaluated for the maximum differential pressure and total deposit volume metrics.

The portion of this task relating to reproducibility was completed via participation in the ASTM Intralaboratory Study (ILS) for the JFTOT experiment. Participation involved two measurements of a newly devised JFTOT Operational Validation Fluid from the ASTM D3241 Reference Fluid Task Force. Both Alcor and Falex brand JFTOT sample tubes were tested, and both measurements were run at 275°C, per the ILS instructions.

Results

1. Repeatability Measurements

Figure 1 presents the maximum deposit thickness and total deposit volume results of the repeatability measurements at 5˚C temperature intervals from 255˚C to 275˚C. The breakpoint of the Richland Jet A, or highest temperature at which the deposit remains below the 85nm max. deposit thickness specification limit, was found to be 265˚C. The maximum deposit thickness results show consistent standard deviation values between temperature settings through 270˚C, but increases drastically at 275˚C. The deposit volume results show a similar trend, but with the decrease in repeatability showing at 270˚C. With both metrics, there are lower deposition levels at 275˚C than 270˚C. This is a sign that the oxidation pathway may become oxygen-limited between these two temperatures. Overall, these metrics provide adequate repeatability for research purposes, with the maximum deposit thickness used in the specification showing a lower standard deviation when 5˚C above the breakpoint temperature.

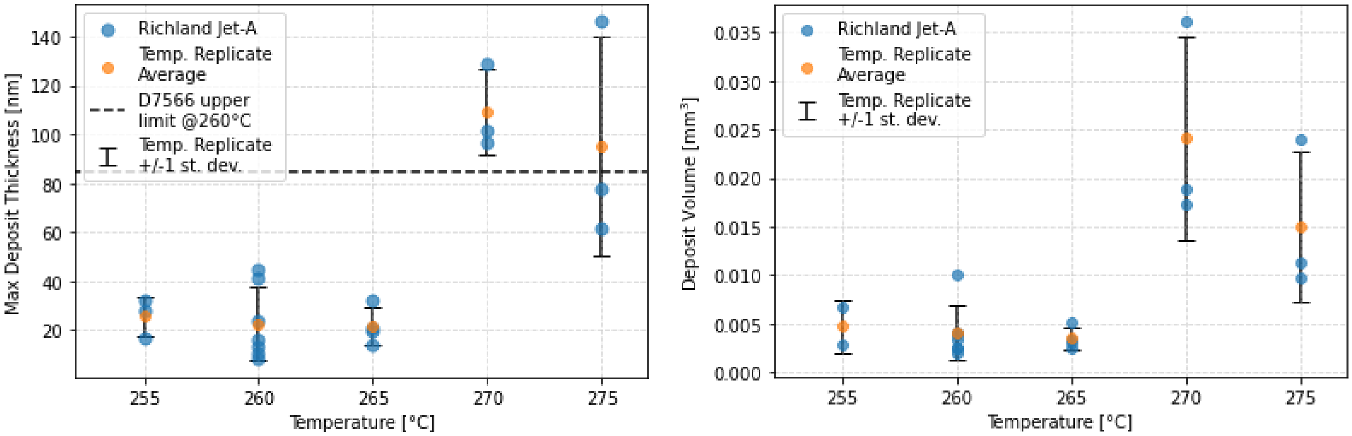

Figure 1. Repeatability measurement maximum deposit thickness (left) and total deposit volume (right) for Richland Jet A at 5˚C intervals from 255˚C to 275˚C.

A third metric recorded during JFTOT testing is the differential pressure (DP). This metric measures the pressure difference across the filter placed on the back end of the sample tube assembly, and is intended to account for insoluble oxidation products that, while not contributing to deposition, are an indicator of thermal oxidative instability. As these products are caught in the filter, the pressure drop increases. A DP greater than or equal to 25mmHg is considered a fail. The DP results for the repeatability measurements are found in Figure 2 below. Unusual oscillating behavior was found for the measurements at 255˚C and 260˚C, where the DP result indicated either 0 or 100mmHg. This poor repeatability makes it

---

® Falex is a registered trademark of Falex Corporation, Sugar Grove, Illinois.

difficult to use the DP data as a pass/fail metric, and given the sensitivity of the ETR compared to the visual tube rating (VTR) previously used in JFTOT research it appears that the deposit thickness is a more reliable metric to rate JFTOT tubes. Documentation of this behavior is important as the 25mmHg maximum DP remains in the ASTM specifications for jet fuels.

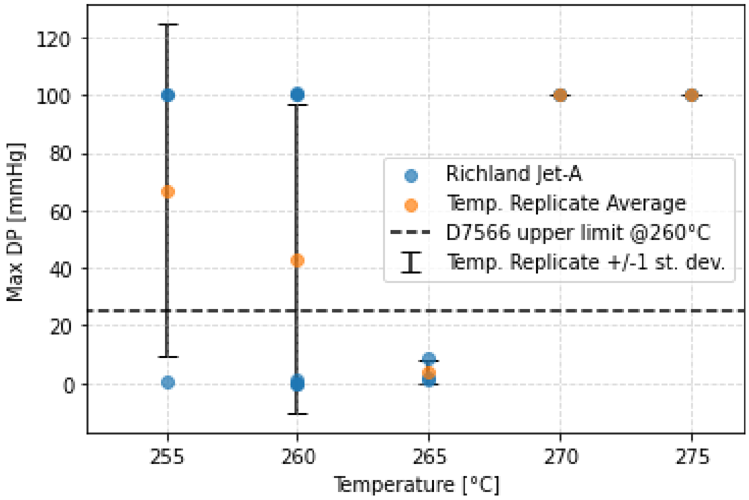

Figure 2. Repeatability measurement maximum differential pressure (DP) for Richland Jet A at 5°C intervals from 255°C to 275°C.

2. Reproducibility Measurements

The results of the ILS are not yet published. The team at WSU was informed that the measurements produced as a part of this work were well within the reproducibility determined by the study.

3. Streaking Phenomenon

While performing breakpoint testing on a second batch of Jet A fuel ("Richland 2 Jet A") an unusual streaking phenomenon appeared on the ETR deposition profile of the JFTOT sample tubes tested at high temperature settings (≥350°C) and persists for new tests <350°C. The repeatable nature of this issue makes it relevant to the work relating to JFTOT repeatability in items 2 and 3 above. This section will chronologically report the discovery of the streaking phenomenon and attempted, but ultimately unsuccessful, mitigation strategies.

Figure 3 and the following two paragraphs present a summary of the testing leading to the tube streaking. A fuel's JFTOT breakpoint is determined by running a series of tests at different temperature settings to determine the highest temperature (+/- 5°C) that a fuel will pass the 85nm maximum deposit thickness and 25mmHg DP spec limits. Richland 2 Jet A performed especially well for a conventional Jet A fuel during breakpoint testing, reporting maximum deposit thickness below 85nm at 330°C (Figure 3, top left), well above the 260°C requirement found in ASTM D1655 (ASTM, 2023a) for petroleum-derived Jet A fuel. This result was also suggested to be accurate by low total nitrogen and sulfur results, <0.5ppm and 48ppm, respectively. A similar result was seen at 325°C (Figure 3, bottom left). Thus, breakpoint testing continued, and the next measurement was made at 350°C.

At 350°C (Figure 3, top center), an asymmetric deposit profile appeared. Interestingly, a separated streak appears upstream on the tube, separate from the primary ridge of deposits, and a gap in the primary ridge is present where the streak would fit. Since noisy data are known to occur in some JFTOT measurements and the deposits did not surpass the 85nm limit, this result was ignored initially, and breakpoint testing proceeded. At 380°C (Figure 3, bottom center), a similar streak appeared upstream on the tube along with a corresponding gap in the primary deposit ridge. Because the primary ridge far exceeded the 85nm specification limit, breakpoint testing continued at a lower temperature. At 360°C (Figure 3, top right), a similar result to the test at 350°C occurred. At this point it was clear that the asymmetric streaking was repeatable. Suspecting high temperature impacts, a test was run at 325°C. These results (Figure 3, bottom right) showed the same anomaly, indicating that some semi-permanent/permanent change had occurred to the instrument.

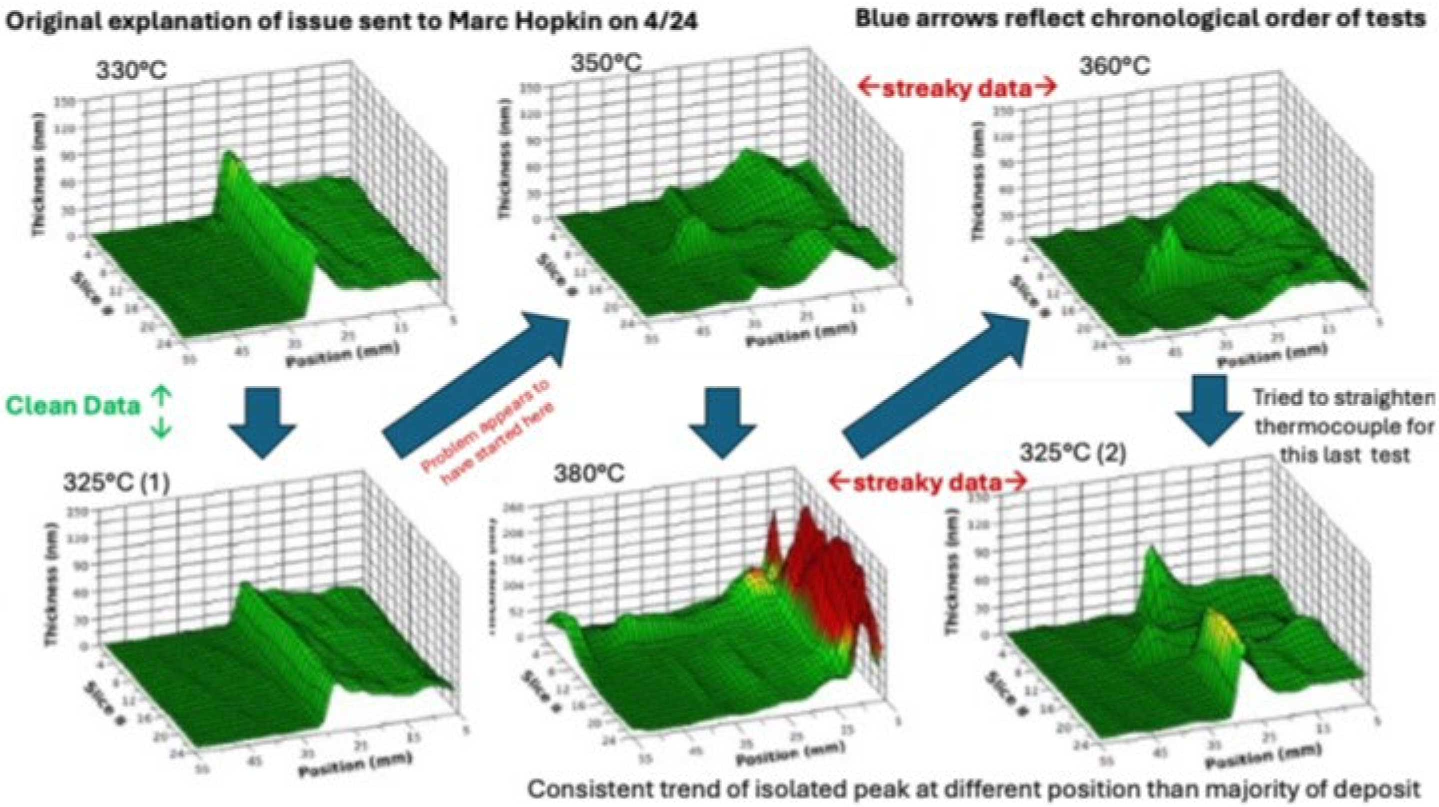

Figure 3. Chronological flowchart summary of streaking phenomenon on Jet Fuel Thermal Oxidation Tester (JFTOT) sample tubes with Richland 2 Jet A.

Once this issue was repeated at previously tested lower temperatures, the process towards reversing or mitigating this issue began. Table 1 contains the experimental variables considered and how we addressed potential problems with said variables. It is important to note that none of these attempts were successful, and the streaking persists at the time of this documentation. The team at WSU has also been in contact with Falex, Inc. (the instrument manufacturer) and George Wilson (retired, previously of Southwest Research Institute) who led the effort to develop the ASTM 3241 JFTOT method.

Table 1. JFTOT experimental variables and attempts to mitigate the asymmetrical streaking. All efforts have been unsuccessful at the time of this report.

JFTOT Experimental Variable	Mitigation Approach
Fuel	• 3 conventional fuels, 4 synthetic blend components (SBC) candidates
Test temperature	• 6 temperature settings
Flow rate	• 3 total flow rate settings: 1.5, 3 (default), and 6 mL/min
Sample tube	• Tube batch number varied • Pre-test uniformity verified in ETR
Sample tube thermocouple	• Thermocouple straightened and lengthwise position varied • Thermocouple replaced • Recalibrated. Both old and new calibration metrics are within recommended range
Sample tube assembly	• Assembly vigorously cleaned, purged between runs with 80/20 petroleum ether/toluene solvent blend • O-rings replaced each run • Entire assembly replaced
Bus bar cooling	• Refreshed with new coolant, removed air bubbles
Internal hardware	• Internal tubing accessed and cleaned • Pump visually inspected

To date since the first occurrence of the streaking, all tests exhibiting any noticeable amount of coking have also displayed the streaking behavior. The engineering team at the manufacturer, Falex, Inc., has not been able to provide a resolution. George Wilson’s observation is that asymmetric flow is common in JFTOT tests, and that he sees no apparent problem in the streaking results. He also provided useful background information and resources, including the notion that the results above 330˚C are likely showing pyrolytic deposits, a far different reaction mechanism than thermal oxidative deposits typically observed by the JFTOT. Thoroughly investigating the streaking phenomenon became an obstacle to continued JFTOT testing (see Task 5) but was necessary to grasp the potential impacts of this on research efforts as well as documenting it as a repeatability risk for the broader community.

Milestone

- Developed understanding of test repeatability and reproducibility.

Major Accomplishments

None.

Publications

None.

Outreach Efforts

George Wilson (Southwest Research Institute, retired) and Falex, Inc., were contacted for feedback about the streaking phenomenon. While not able to resolve the issue, both provided useful feedback to investigate and/or rule out several potential causes, including fuel flow properties, thermal gradients, and additional maintenance procedures not performed during routine care of the instrument.

Awards

None.

Student Involvement

Conor Faulhaber, a PhD student at WSU, leads JFTOT-related experimental work for the lab including test planning, data organization, data analysis, instrument maintenance, and reporting results. Kaamel Sidiqi, an undergraduate at WSU, is trained on and runs the JFTOT experiment.

Plans for Next Period

Continue to monitor the streaking phenomenon. Assess repeatability of doped samples.

References

ASTM International. (2023a). *ASTM D1655-22a: Standard Specification for Aviation Turbine Fuels.* https://doi.org/10.1520/D1655-22A

ASTM International. (2023b). *ASTM D3241-23: Standard Test Method for Thermal Oxidation Stability of Aviation Turbine Fuels.* https://doi.org/10.1520/D3241-23

Task 2 – Gain Proficiency in Analytical Methods for Trace Impurities Detection

Washington State University

Objective

The objective of Task 2 is to become skilled in performing the experimental methods required to detect the trace impurities responsible for thermal oxidation in jet fuels. This task requires equipment installation, lab personnel training, and in-house method development to master the application of interest.

Research Approach

The main subject of this work was to detect fuel-bound sulfur, nitrogen, and oxygenated species in jet fuel, as well as trace metals. The following sub-sections detail the different analytical methods employed for each type of impurity.

Sulfur-Containing Compounds

Sulfur-containing compounds (SCC) are being detected with three different methods: ultraviolet fluorescence (UVF), inductively coupled plasma optical emission spectrometry (ICP-OES), and combustion ion chromatography (CIC). Multiple methods were developed for sulfur detection due to its prevalence in conventional jet fuel pathways and because, in addition to thermal stability, there is significant research interest in the quantification of parts-per-billion levels of sulfur for its impact on contrails: ice particle count and size distribution (Karcher, 1998). Comparisons of these methods to each other contributes to the evaluation of these methods and builds confidence in results near the detection limit.

1. **Ultraviolet Fluorescence**

The UVF system quantifies total sulfur by converting sulfur-containing compounds into sulfur dioxide (SO_2) in an oxygen-rich combustion environment. The generated SO_2 absorbs ultraviolet light in the 200–400 nm range and subsequently emits fluorescence (~330 nm) upon relaxation. This fluorescence is detected using a photomultiplier tube, and the resulting signal is integrated to calculate the total sulfur content of the original sample. The signal intensity is directly proportional to the sulfur concentration, allowing for quantitative analysis via linear regression of standard concentrations versus integrated signal area.

UVF results were benchmarked against ASTM D5453 (ASTM, 2025), a standard method for determining total sulfur in the range of 1.0 to 8000 mg/kg. ASTM D5453 is widely regarded for its ability to convert all sulfur species into SO_2, thereby minimizing matrix effects and enhancing accuracy. This method is preferred for regulatory compliance monitoring due to its high sensitivity and reliability, and is referenced in the jet fuel specifications, ASTM D1655 (ASTM, 2023a), D7566 (ASTM, 2024d), and D4054 (ASTM, 2024b), for this reason. For UVF sulfur detection, the WSU SAF Lab uses XPLORER-TS.® The

---

® XPLORER-TS is a registered trademark of TE Instruments, Houston, Texas.

instrument settings are as follows: 100 mL/min argon flow rate, 300 mL/min primary oxygen flow rate, 100 mL/min collision oxygen flow rate, 1000°C furnace temperature. The instrument is calibrated using eight internal standards of dibenzothiophene (98% purity) doped in n-dodecane (>99% purity) for three different sulfur content ranges: 0 – 100 mg/kg, 0 – 12 mg/kg, and a low-sulfur calibration from 0 – 1.58 mg/kg. Each calibration curve maintains $R^2 > 0.999$ (R^2: coefficient of determination).

2. Inductively Coupled Plasma Optical Emission Spectroscopy

ICP-OES is an analytical technique that uses a high-temperature plasma to excite atoms and ions, causing them to emit electromagnetic radiation at element-specific wavelengths. The intensity of this emitted light is directly proportional to the concentration of each element in the sample.

In a typical ICP-OES setup, the liquid sample is introduced via a nebulizer, which generates an aerosol that is carried by an argon gas stream into an argon plasma operating at approximately 10,000 K. Within the plasma, the sample components are atomized and excited. As the excited atoms and ions return to their ground state, they emit light at characteristic wavelengths. An optical system, typically equipped with a polychromator, disperses this light and measures the emission intensity at each relevant wavelength. These intensities are then correlated to elemental concentrations through calibration.

ASTM D7111 (ASTM, 2021) is a standard method developed to quantify trace levels of metallic elements in middle distillate fuels (e.g., diesel, kerosene, jet fuel). However, analyzing petroleum-based samples presents several analytical challenges. One major issue is the requirement for matrix-matched calibration standards—the calibration curve must be prepared using a solvent mixture that closely mimics the fuel sample matrix. Due to the complex and variable composition of fuel samples, creating a suitable matrix-matched standard is not straightforward.

The method also recommends the use of internal standards to correct for matrix effects and instrumental drift. However, care must be taken to avoid wavelength overlap, which can lead to spectral interference or false positives due to signal contributions from other elements. The hydrocarbon matrix can significantly influence signal behavior, either suppressing or enhancing emission intensities, further complicating quantitative analysis. Moreover, the volatility and flammability of the organic solvents used in sample preparation demand strict adherence to safety protocols.

To mitigate these challenges, ASTM D7111 outlines specific strategies, including the use of matrix-matched calibration standards, internal standardization for signal normalization, controlled sample introduction rates to maintain plasma stability and analytical precision. Although ICP-OES is traditionally applied to the quantification of metals under ASTM D7111, we have adapted this method for sulfur determination in organic fuel samples. This adaptation is motivated by several published studies that demonstrate the feasibility of ICP-OES for sulfur quantification in oil matrices, prompting us to validate this approach for our application.

The instrument settings for the WSU SAF Lab ICP-OES sulfur detection method are as follows: 181.669 nm wavelength, 0.61 L/min nebulizer flow, 12.0 L/min plasma flow, and 25% oxygen flow. A-solv, Agilent®'s commercial kerosene solvent, is used as the calibration solvent for matrix-matching purposes. This limits the ICP-OES analysis method's sensitivity, as A-solv contains some baseline sulfur content (~1mg/kg). Investigating other matrix-matched solvents with lower sulfur levels will be part of the future work with this instrument. The ICP-OES method was calibrated for sulfur measurement using two calibration curves produced with sulfur compounds doped into A-solv, one with dodecanethiol (0.25–50 mg/kg) and another with dibenzothiophene (0.27 – 9.3 mg/kg). Both curves demonstrated $R^2 > 0.999$

3. Combustion Ion Chromatography

The CIC method includes a combustion and sample introduction unit and an ion chromatography (IC) system. Sulfur in the sample is converted to sulfur oxides (SO_x) (mainly SO_2 and sulfur trioxide [SO_3]) in a high-temperature combustion furnace at approximately 1000˚C in a pure oxygen atmosphere. The combustion gases are transferred into an absorption solution, typically a hydrogen peroxide solution where SO_2 and SO_3 dissolve to form sulfurous acid (H_2SO_3) and sulfuric acid (H_2SO_4) and sulfite ion (SO_3^{2-}) further oxidizes to sulfate (SO_4^{2-}). The aqueous containing anions such as sulfate is injected into an ion chromatography system. The IC column separates the ions based on their charge and size. The separated ions are detected using suppressed conductivity detection, a sensitive method that enhances signal by reducing background conductivity from the eluent.

® Agilent is a registered trademark of Agilent Technologies, Inc., Santa Clara, California.

The scope of ASTM D7359 (ASTM, 2023d), the standard method for halide and sulfur detection via CIC, is 0.1–10 ppm per element. For sub-ppm detection, special attention must be given to contamination control and system cleanliness. Our system was optimized by reducing sample injection (60uL) volume to minimize soot formation and extending measuring tubing (aqueous sampling, 200uL) to improve signal-to-noise ratio. The WSU SAF Lab method for CIC sulfur measurement uses the following conditions: 200 mL/min argon flow rate, 400 mL/min oxygen flow rate, 100 mL/min working standard argon flow rate, 8 mL absorption solution volume, Dionex® IonPac® AS19 250mm x 4mm ion chromatography column, 50mm x 4mm guard column, 20mM potassium hydroxide (KOH) eluent, and a 1.0 mL/min sample flow rate. Multiple calibration curves were developed and compared for the CIC using dodecanethiol, benzothiophene, dibenzothiophene, and di-tert-butyldisulfide doped in n-dodecane at concentrations ranging from 0 to 14ppm. While the slope and intercept for each dopant's curve varied slightly, all reported $R^2 > 0.999$.

4. Results

Table 2 below depicts the detection (i.e., limit of detection [LOD]) and quantification (i.e., limit of quantitation [LOQ]) limits determined for each of the sulfur quantification methods discussed. The results indicate that the UVF method exhibits slightly better sensitivity than the CIC method, with the ICP-OES method far behind the other methods. This is likely due to the need for matrix-matching calibration for the ICP-OES method, making it difficult to find a high-purity solvent to establish a low-sulfur baseline. In addition to having desirable sensitivity, the UVF method is also the simplest instrument to operate and maintain, making it the first choice for sulfur quantification efforts. Interestingly, the standard for this method, ASTM D5453, bounds the application of UVF to sulfur levels between 1.0 and 8,000 mg/kg. Thus, it was necessary to verify the sub-ppm UVF sulfur measurements with the CIC method. Additionally, the CIC method more directly measures sulfur content compared to the UVF method. Because the UVF detector captures signal across a range of UV wavelengths, overlapping UV signal from the hydrocarbon content making up over 99% of jet fuel samples can create a false sulfur signal that becomes significant for fuels with little sulfur content. The ion chromatography avoids this issue, as hydrocarbons will not elute with a sulfate ion peak. While it is a more complex experiment to run and maintain, this makes the CIC method a dependable choice for gaining confidence in low-sulfur measurements, including verifying the sulfur content in low-sulfur standards used to calibrate other experiments.

Table 2. Sulfur detection method limit of detection (LOD) and limit of quantitation (LOQ), determined by 3x and 10x, respectively, of the standard deviation of 7 instrument blanks.

Sulfur Detection Method	LOD [mg/kg]	LOQ [mg/kg]
UVF	0.024*	0.098*
ICP-OES	0.5	1.5
CIC	0.04	0.1

**Approximation based on the 0 – 12 mg/kg calibration curve. In practice LOD/LOQ is determined directly from signal area. Also, see discussion around Figure 5 for context surrounding these values.*

Figure 4 shows the results of a set of sulfur measurements on a set of Hydroprocessed Esters and Fatty Acids (HEFA) fuel samples used in a flight test, external to this project. The UVF and CIC results display good agreement across the range of samples, remaining within 5% relative standard deviation (RSD) of each other. Meanwhile, the ICP-OES results appear systematically lower than the other methods. Additionally, as shown by the black lines, the repeatability for the ICP-OES method exceeds 10% RSD while the UVF and CIC methods report values of 0.069 – 1.18% and 0.063 and 1.13% RSD, respectively. Both the agreement between UVF and CIC methodologies and the good repeatability at low sulfur concentrations confirm that they are more than suitable for the application of jet fuel sulfur quantification.

® Dionex and IonPac are registered trademarks of Dionex Corporation, Sunnyvale, California.

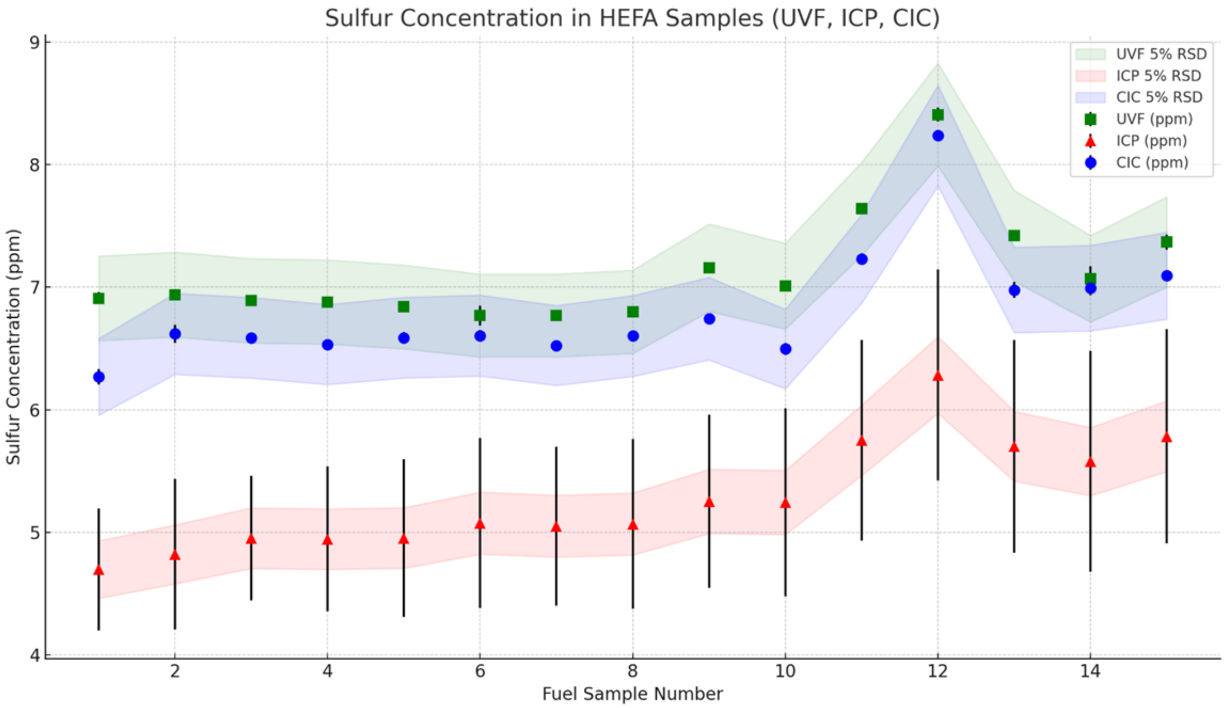

Figure 4. Ultraviolet fluorescence (UVF), inductively coupled plasma optical emission spectrometry (ICP-OES), and combustion ion chromatography (CIC) sulfur quantification results for 15 hydroprocessed esters and fatty acids (HEFA)-synthetic paraffinic kerosene (SPK) fuel samples. The shaded region reflects 5% relative standard deviation (RSD) for each test, and the black bars indicate the RSD of three replicate measurements on each sample.

After deeming the UVF and CIC methods suitable for jet fuel sulfur quantification, including sub-ppm-level detection, 6 SAFs with suspected low sulfur content were selected for testing. The results of this work are shown below in Figure 5. Here, the UVF measurements consistently overshoot those of the CIC method. This is suspected to be a result of the chemistry involved with each detection method, as mentioned before. At sub-ppm sulfur levels, the small amount overlapping ultraviolet wavelength from the bulk hydrocarbons become significant to the overall signal captured by the UVF detector. On the other hand, there is no hydrocarbon interference in the sulfate ion peak on the IC chromatograph, so the sulfur content is measured more directly than in the UVF method, and the result is consistently lower. Using the CIC method, the calibration blank n-dodecane can be analyzed for its baseline sulfur content, and the UVF calibration can then be adjusted. However, because the LOD and LOQ are derived from instrument blank values, they are not corrected in the UVF and ignore the impact of blank interference. Thus, the LOD and LOQ values for the UVF method in Table 2 likely overestimate the instruments sensitivity. The extent of this overestimation is yet to be determined and may also depend on the composition of the bulk hydrocarbon matrix. Still, its ease of use and good repeatability makes the UVF method a valuable tool for sulfur quantification.

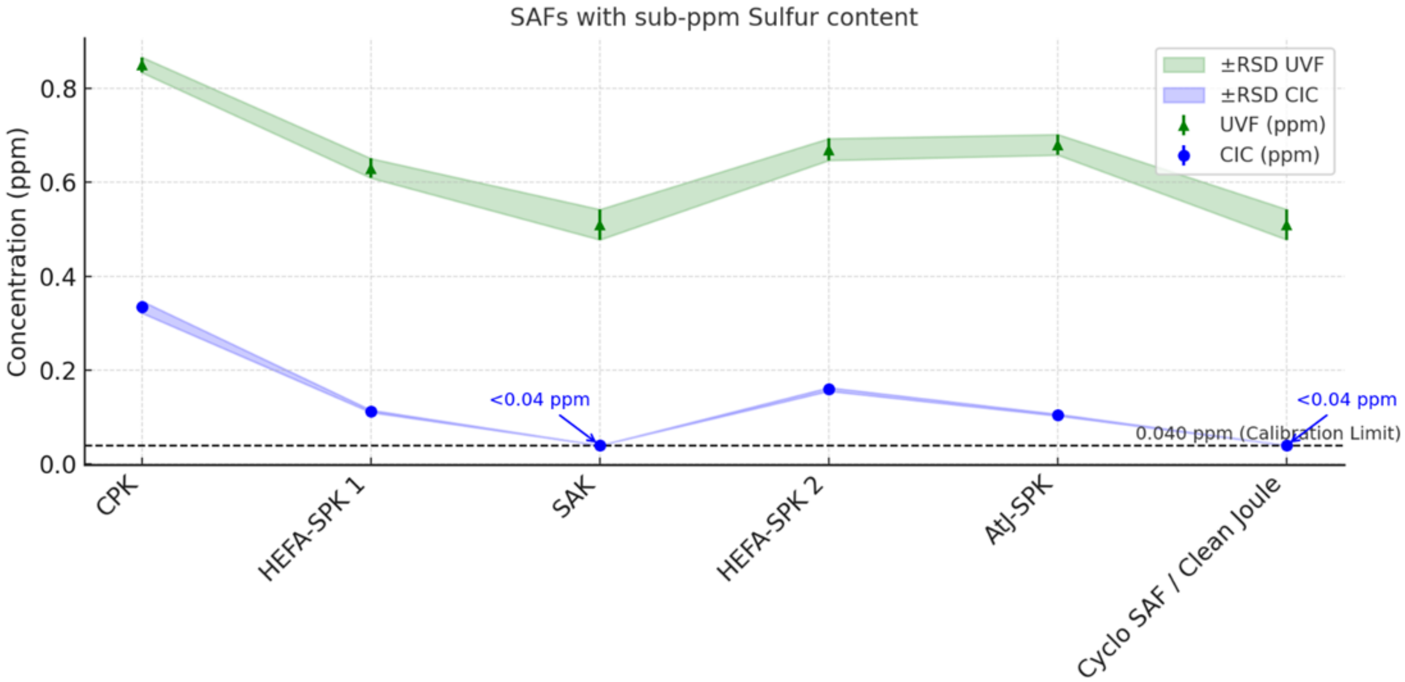

Figure 5. Low-sulfur measurement results from ultraviolet fluorescence (UVF) (green) and combustion ion chromatography (CIC) (blue) test methods. The shaded regions reflect the measured standard deviation for 3 replicates of each sample. Note that synthesized aromatic kerosene (SAK) and CycloSAF were measured below the CIC limit of detection of 0.04 mg/kg.

Mercaptan Sulfur

In addition to total sulfur content, mercaptan sulfur is also called out in the jet fuel specification. The WSU SAF Lab maintains the capability to run ASTM D3227 (ASTM, 2023b), a potentiometric method for quantifying mercaptan sulfur in jet fuel samples.

Nitrogen-Containing Compounds

Nitrogen-containing compounds (NCC) are quantified using 1-dimensional gas chromatography-nitrogen chemiluminescence detection (GC-NCD). The WSU SAF Lab runs this instrument as an adapted version of ASTM D4629 (ASTM, 2017), which sends the sample directly from the combustor to the detector rather than separating it through a gas chromatography (GC) column first. The added advantage of the GC-NCD is that individual nitrogen species can be evaluated on boiling point or polarity, depending on the type of column used. This can aid with further identification via solid-phase extraction (SPE) coupled with gas chromatography-mass spectrometry (GC-MS) that will be described in Task 3 of this document. After several iterations of method development using the work of Deese et al. (2020) as a starting point, Gaussian peak shapes and acceptable sensitivity were achieved. The resulting GC-NCD conditions can be found in Table 3.

Table 3. Gas chromatography-nitrogen chemiluminescence detection (GC-NCD) conditions determined via method development.

GC-NCD Variable	Setpoint
Inlet Temperature	300°C
Inlet Pressure	3.3573 psi
Total Flow	20.6 mL/min
Septum Purge Flow	3 mL/min
Inlet Mode	Split
Split Ratio	10:1
Carrier Gas	Helium
Column	HP-5, 30m x 0.320mm x 0.250micron
Column Flow	1.6 mL/min
Column Pressure	3.3573 psi
Average Velocity	43.907 cm/sec
Holdup Time	1.1388 min
Oven Program	Start at 60°C and hold 2 min. Ramp 25°C/min to 160°C hold 2.3min. Ramp 20°C/min to 300°C, no hold.
NCD Base Temperature	280°C
NCD Burner Temperature	900°C
Hydrogen Gas Flow	4 mL/min
Oxygen Gas Flow	8 mL/min

The NCD burner is fed with pure hydrogen (H_2) and oxygen (O_2), such that any nitric oxide (NO) produced is the result of the combustion of nitrogenated species in the sample. The nitrogen chemiluminescence method works by reacting NO with generated ozone, resulting in excited nitrogen dioxide (NO_2^*). When this returns to its ground state NO_2, the emitted red/infrared light is detected and can be directly related to the nitrogen content in the sample. However, similar to the UVF method for sulfur detection, the bulk hydrocarbon content of the fuel can contribute to some overlapping light emission that is captured by the detector. According to Agilent, the ratio of carbon signal to that of a nitrogen compound is $1{:}10^7$, meaning that there can be noticeable interference depending on the hydrocarbon matrix and the amount of individual nitrogen compounds. To probe this, GC-NCD calibration curves were produced using several purchased nitrogen compounds doped individually in a number of low-boiling point solvents, including n-hexane, isopropyl alcohol, and acetone. It was found that calibration curves were consistent between nitrogen compounds and solvents as long as coelution did not take place. An example of one of these calibration curves is found in Figure 6 below.

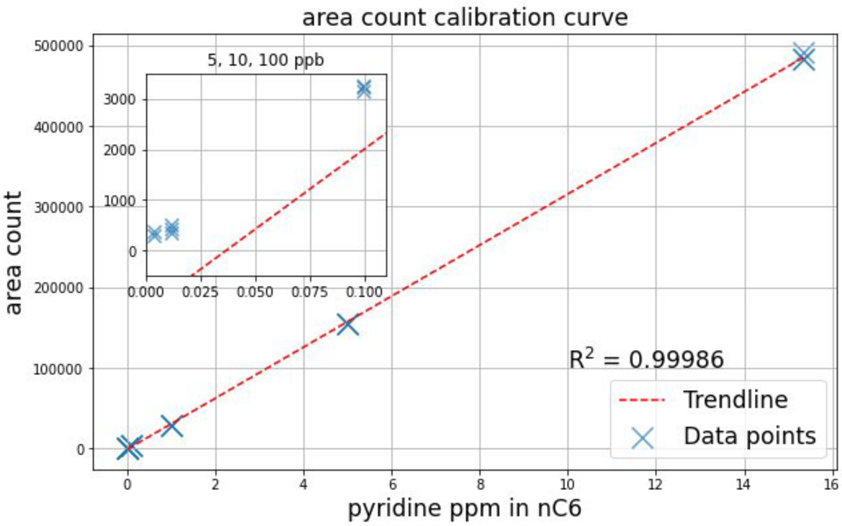

Figure 6. Gas chromatography-nitrogen chemiluminescence detection (GC-NCD) calibration curve with pyridine doped in n-hexane. This graph is one of several calibration curves produced during method development and may not reflect the exact curve used to calculate nitrogen content.

While it did not prove to cause significant issues for calibration, the interfering carbon signal was found to cause some baseline-related problems with more complex fuels. Figure 7 below shows a zoomed-in portion of overlapping GC-NCD chromatograms from fuels sampled sequentially in a continuous run process as hydrodenitrification (HDN) were increased over time. Calling attention to the signal at approximately 2.145 min retention time, these peaks are roughly Gaussian and noticeably decrease in size with each sampling. This indicates that these are likely true nitrogen peaks given the context known about the samples. Comparatively, the "peaks" prior to the 2.145 min mark are misshapen and appear to remain consistent between samplings. With knowledge of the HDN process, the WSU SAF Lab was able to determine that these "peaks" are actually the interfering signal from the bulk hydrocarbon species at high concentration in the fuel. Since the HDN targets nitrogen species, this part of the signal remains the same between samplings. This was an important discovery for the team, as the sequentially sampled fuels allowed for the overlaid comparison. In most GC-NCD use cases, there is little reference outside of rough peak shape to determine whether or not a small peak is an NCC or some carbon interference. One way to circumvent this, which takes additional fuel volume, is to perform solid-phase extraction to amplify the true polar NCC peaks away from the baseline. This method is discussed in Task 3. Additionally, changing column type to a mid-polar phase may help to isolate the non-polar carbon signal to one end of the chromatogram that can be ignored during analysis. Investigating this is part of the next steps in progressing the GC-NCD method.

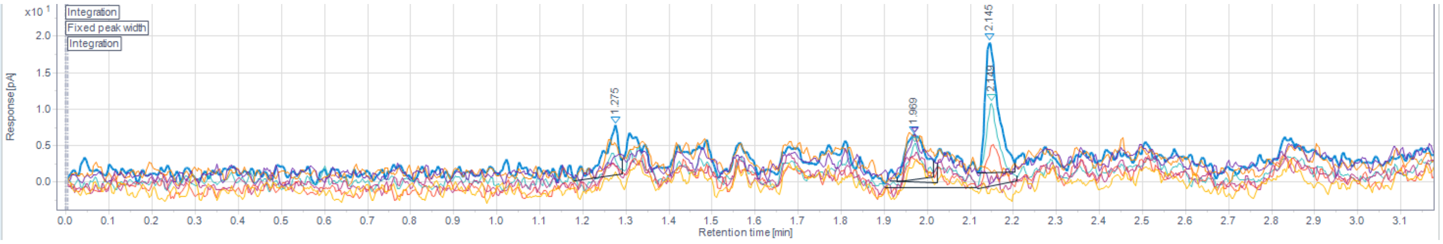

Figure 7. Overlaid and cropped gas chromatography-nitrogen chemiluminescence detection (GC-NCD) chromatograms for fuels sampled sequentially during a continuous run experiment where HDN levels were increased over time.

Oxygen-Containing Compounds

The ASTM D3242 (ASTM, 2023c) potentiometric method for acidity measures total acidity but, by inference, it is reasonable to assign all of the acidity to carboxylic acids. Similarly, peroxides are detected via the ASTM D3703 (ASTM, 2024a) potentiometric method. Esters can be measured via ASTM D7871 (ASTM, 2023c) which employs infrared (IR) spectroscopy to interrogate the carbonyl stretch of effluent passing through a high-pressure liquid chromatographer. Alcohol and ethers are harder to characterize. Lastly, impurities amplification methods have been found to be useful for oxygen-containing compounds (OCC) identification via solid phase extraction and gas chromatography-mass spectrometry (SPE-GC-MS). This is described in detail in Task 3 below. All of these strategies have been developed and utilized in the WSU SAF Lab for jet fuel analysis.

Olefins
Along with polar OCCs, olefins are also able to be quantified via ASTM D1319 (ASTM, 2020a). Additionally, WSU SAF Lab personnel are trained in the ASTM D2710 test method (ASTM, 2020b) for Bromine index, a method for evaluating olefin content in jet fuels.

Trace metals
Trace metals are quantified via ICP-OES according to ASTM D7111. This method is the same as that of sulfur detection with the same instrument but largely avoids the matrix-matching issue that was previously discussed. The A-solv matrix has little-to-no baseline metals content, which provides better sensitivity when calibrating on trace metals standards. The improved sensitivity allows for detection down to the specification limit of 0.1 mg/kg for 22 metals listed in ASTM D7566.

Amongst the metals regulated by jet fuel specifications, copper is known as a significant thermal stability risk for fuels. For that reason, it is further limited to 20 ppb in novel jet fuel pathways going through ASTM D4054 evaluation. The WSU SAF Lab personnel have been trained to operate a graphite furnace-atomic absorption spectrometer for the detection of copper at parts-per-billion levels via the ASTM D6732 method (ASTM, 2024c).

Milestones

- Gained at least some proficiency in execution of the experiments necessary to characterize all of the most common or important impurities that may be found in sustainable or petroleum jet fuel components.
- Advanced the state-of-the-art measurement capability for ultra-low levels of sulfur in jet fuels.

Major Accomplishments

None.

Publications

None published. Journal article evaluating the three sulfur detection methods is in progress. Submission to ACS *Precision Chemistry* Journal is expected in Spring 2026.

Outreach Efforts

None.

Awards

None.

Student Involvement

Conor Faulhaber, a graduate student at WSU, leads the development of the nitrogen and sulfur detection methods and is involved in the reporting of this material. Kaamel Sidiqi, an undergraduate at WSU, is trained on and operates the GC-NCD and UVF sulfur instruments and assists with data organization for these tests. Patricia Garcia-Alfaro, another undergraduate at WSU, is trained on and operates the CIC sulfur instrument. She also developed a standard operating procedure for the CIC method.

Plans for Next Period

- Complete a publication on low-sulfur detection methods.
- Improve the GC-NCD method for fuels resulting in a noisy baseline.

References

ASTM International. (2017). *ASTM D4629-17: Standard Test Method for Trace Nitrogen in Liquid Hydrocarbons by Syringe/Inlet Oxidative Combustion and Chemiluminescence Detection.* https://doi.org/10.1520/D4629-17

ASTM International. (2020a). *ASTM D1319-20a: Standard Test Method for Hydrocarbon Types in Liquid Petroleum Products by Fluorescent Indicator Adsorption*. https://doi.org/10.1520/D1319-20A

ASTM International. (2020b). *ASTM D2710-20: Standard Test Method for Bromine Index of Petroleum Hydrocarbons by Electrometric Titration*, PA May 1, 2020. https://doi.org/10.1520/D2710-20

ASTM International. (2021). *ASTM D7111-16 (Reapproved 2021): Standard Test Method for Determination of Trace Elements in Middle Distillate Fuels by Inductively Coupled Plasma Atomic Emission Spectrometry.* https://doi.org/10.1520/D7111-16R21

ASTM International. (2023a). *ASTM D1655-22a: Standard Specification for Aviation Turbine Fuels.* https://doi.org/10.1520/D1655-22A

ASTM International. (2023b). *ASTM D3227-23: Standard Test Method for (Thiol Mercaptan) Sulfur in Gasoline, Kerosine, Aviation Turbine, and Distillate Fuels (Potentiometric Method).* https://doi.org/10.1520/D3227-23

ASTM International. (2023c). *ASTM D3242-23: Standard Test Method for Acidity in Aviation Turbine Fuel.* https://doi.org/10.1520/D3242-23

ASTM International. (2023d). *ASTM D7359-23: Standard Test Method for Total Fluorine, Chlorine, and Sulfur in Aromatics Hydrocarbons and Their Mixtures by Oxidative Pyrohydrolytic Combustion followed by Ion Chromatography Detection (Combustion Ion Chromatography-CIC).* https://doi.org/10.1520/D7359-23

ASTM International. (2023e). *ASTM D7871-23: Standard Test Method for Analysis of Cyclohexane by Gas Chromatography (Effective Carbon Number).* https://doi.org/10.1520/D7871-23

ASTM International. (2024a). *ASTM D3703-18 (Reapproved 2024): Standard Test Method for Hydroperoxide Number of Aviation Turbine Fuels, Gasoline, and Diesel Fuels.* https://doi.org/10.1520/D3703-18R24

ASTM International. (2024b). *ASTM D4054-24d: Standard Practice for Evaluation of New Aviation Turbine Fuels and Fuel Additives.* https://doi.org/10.1520/D4054-24

ASTM International. (2024c). *ASTM D6732-04 (Reapproved 2020): Standard Test Method for Determination of Copper in Jet Fuels by Graphite Furnace Atomic Absorption Spectrometry.* https://doi.org/10.1520/D6732-04R20

ASTM International. (2024d). *ASTM D7566-24d: Standard Specification for Aviation Turbine Fuel Containing Synthesized Hydrocarbons.* https://doi.org/10.1520/D7566-24D

ASTM International. (2025). *ASTM D5453-25: Standard Test Method for Determination of Total Sulfur in Light Hydrocarbons, Spark Ignition Engine Fuel, Diesel Engine Fuel, and Engine Oil by Ultraviolet Fluorescence.* https://doi.org/10.1520/D5453-25

Deese, R.D., Morris, R.E., Romanczyk, M., Metz, A.E., Loegel, T.N. (2020). Nitrogen Compound Characterization in Fuels by Multidimensional Gas Chromatography. *Journal of Visualized Experiments, 159*. https://doi.org/10.3791/60883

Karcher, B. (1998). On the potential importance of sulfur-induced activation of soot particles in nascent jet aircraft exhaust plumes. *Atmospheric Research, 46*, 293 – 305. https://doi.org/10.1016/S0169-8095(97)00070-7

Task 3 – Develop Methods for Natural Impurities Amplification

Washington State University

Objective

The objective of Task 3 is to experimentally increase the concentration of the natural impurities of a jet fuel, conventional or synthetic, into a polar extract. The reason for this is twofold. First, the increased concentration of trace impurities improves the resolution of peaks in GC-MS analysis for the purposes of identification. Second, a polar extract isolated from the solvent used for extraction allows for doping studies using the natural impurities profile of the fuel. Doing so for thermal stability, as will be discussed in Tasks 4 and 5, may provide more relevant information compared to that of doping studies with individual molecules on the extent of refining required to meet thermal stability standards. If isolation from the extracting solvent is a problem, the improved identification capabilities with the extracted impurities better inform future doping studies with cocktails of purchased impurities made to approximate naturally occurring impurities.

Research Approach

To accomplish this goal, a common fuel analysis technique known as solid-phase extraction (SPE) was employed to separate the polar impurities of a fuel from the bulk hydrocarbon matrix (Link et al., 2005 & 2007). Previous work on this project performed liquid-liquid extraction on fuels using methanol to achieve the same goal. However, after experience with that method, the removal of large quantities of methanol proved difficult and the isolation of trace impurities as discussed in Task 2 from the aromatic fraction of the fuel is easier under SPE. For this reason, the work in this period of performance was dedicated towards refining the SPE methodology.

SPE works in a 4-step process outlined in Figure 8 below. The SPE is performed by the WSU SAF Lab using a 6mL, 500mg silica bed Thermo Fisher Scientific® Hypersep® cartridge. First, the cartridge is conditioned using 5 mL of n-heptane. This homogenizes the silica bed and washes out any loose particulates. Then, the sample is introduced. Depending on the impurity concentration in the sample, anywhere from 5 to 50 mL of sample may be needed to achieve adequate resolution in GC-MS analysis. Next, the remainder of the non-polar hydrocarbons in the sample are washed out of the silica bed using n-heptane while the polar impurities stick to the silica. An example of this can be seen on the right side of Figure 7, where oxidation products in a trans-decalin sample are seen as a thin dark line in the silica bed. Up to two times the amount of sample is needed in n-heptane to wash out the aromatic content of fuels, as these molecules are slightly polar and can be difficult to remove from the silica bed. Lastly, the polar analytes are eluted using a methanol rinse and are collected into a vial for further analysis. A volume of 1-2 mL methanol, depending on sample impurity concentration, is ideal to maintain a high concentration of polars in the extract for the best possible resolution.

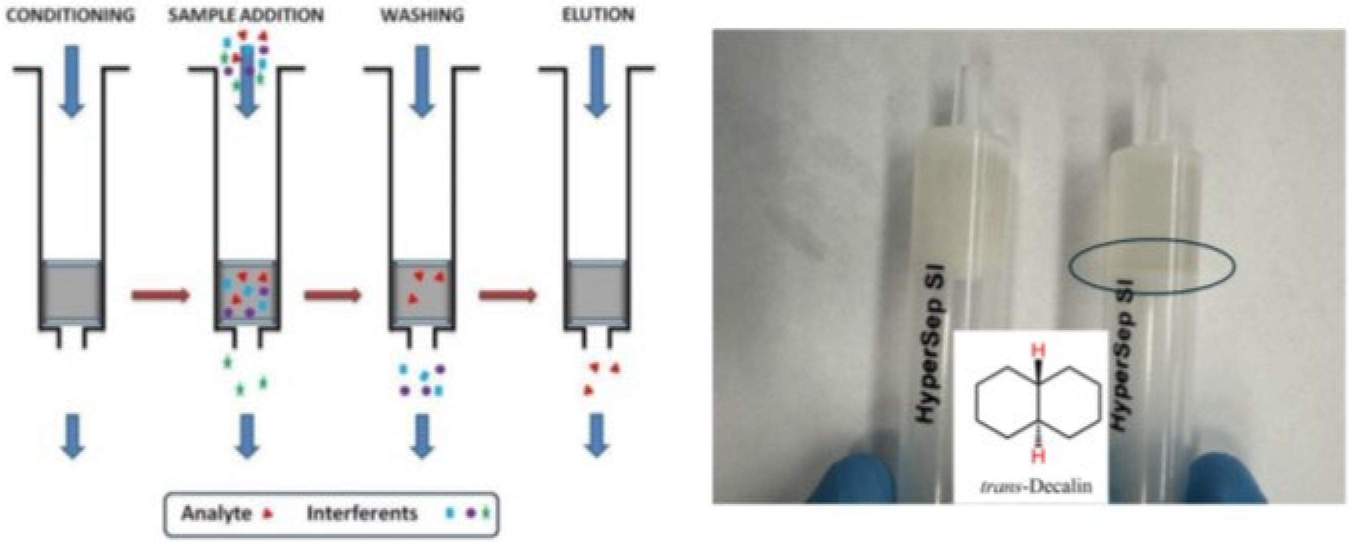

Figure 8. Graphical description of the SPE process (left) and a comparison of two SPE cartridges (right) with the left cartridge representing a clean, conditioned silica bed and the right showing the oxidation products of an aged trans-decalin sample as a dark line in the silica bed (circled).

For a separate ongoing project, ignition delay measurements taken with the aged trans-decalin sample were inconsistent with literature values, and oxidation was suspected as the culprit (Yang et al., 2025). SPE was performed to “clean” the trans-decalin sample, and the polar extract was analyzed in the GC-MS for validation of this procedure. Figure 9 below features the GC-MS chromatogram of said extract shown on the right side of Figure 8. The primary peak was identified as trans-decalin, as expected. Further along the x-axis, smaller peaks of oxidized derivatives of trans-decalin were identified in the MS Library, indicating that polars had been successfully extracted from the sample. To reinforce this result, the ignition delay result for the cleaned trans-decalin sample was consistent with literature data.

® Thermo Fisher Scientific and Hypersep are registered trademarks of Thermo Fisher Scientific, Inc., Waltham, Massachusetts.

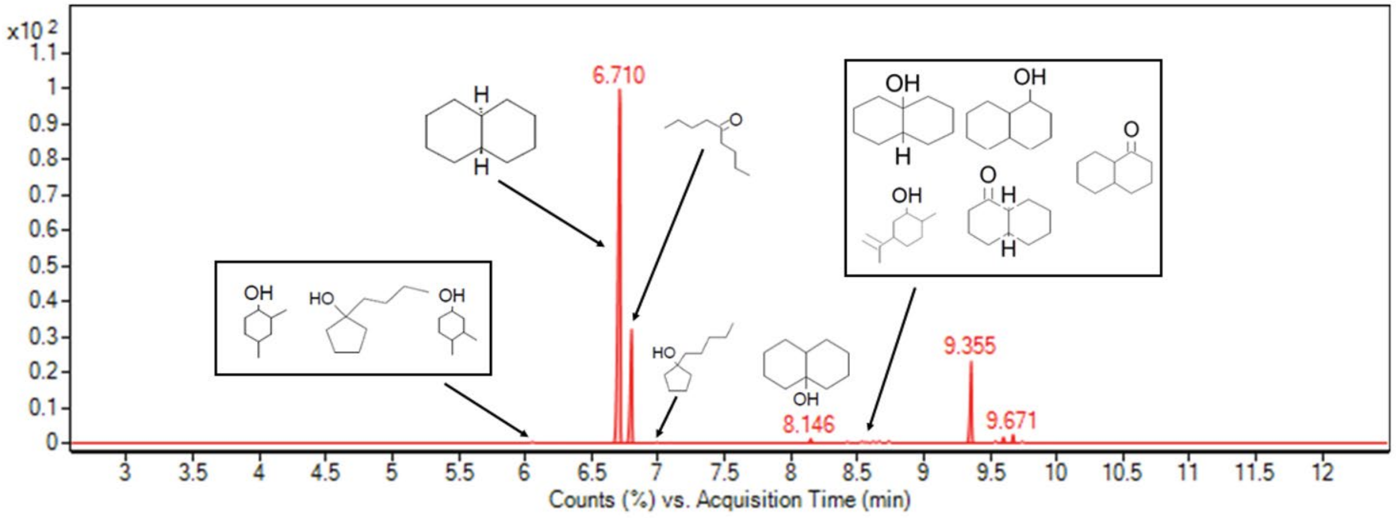

Figure 9. GC-MS chromatogram of aged trans-decalin solid-phase extraction (SPE) extract. Callouts show molecular structure of peaks identified in the MS Library.

Figure 10 provides an example of further application of this method. This time, rather than a neat molecule, SPE was performed on a complex SAF candidate to determine its polar impurity profile. On the left is the bulk hydrocarbon distribution of this fuel, and on the right is the GC-MS result of the SPE extract. The peaks in the GC-MS chromatogram were identified as mostly phenolic compounds, which are known to impact thermal stability in fuels (Link et al., 2005). For this synthetic fuel, the impurity profile is very specific. However, for more complex pathways, including conventional petroleum fuels, the impurity profile is broader and can cause difficulties in identification efforts. This can be seen in Figure 11, where the significant number of overlapping peaks indicates poorer separation and results in poor matches in the MS Library. Future work on this method may include adjusting GC-MS hardware and/or method programming to improve separation. Additionally, while not shown here, the plethora of impurities quantification tools outlined in Task 2 can help to characterize these SPE extracts.

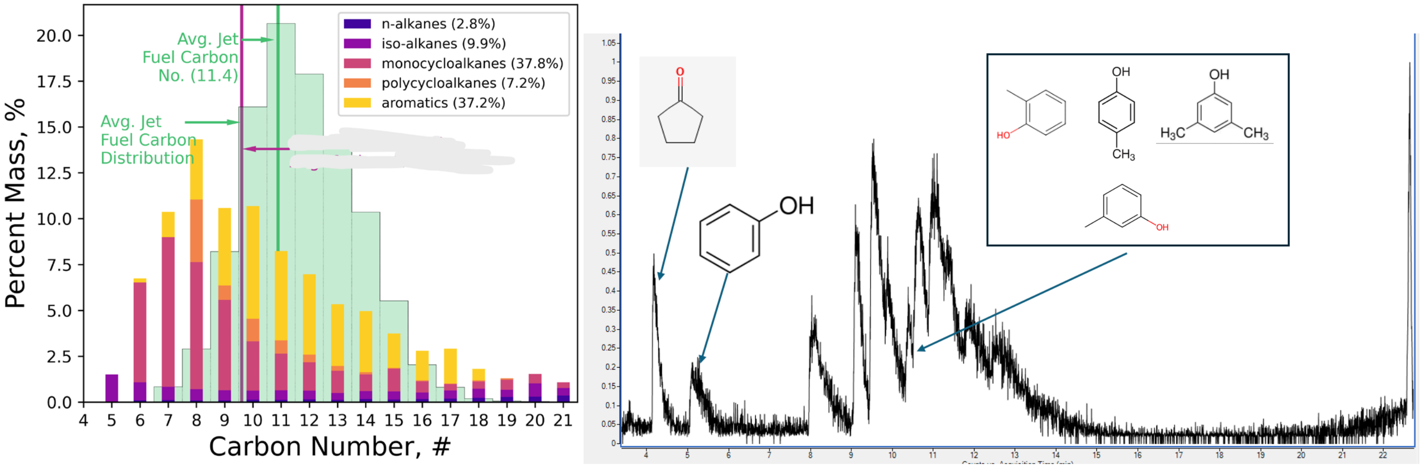

Figure 10. Bulk hydrocarbon distribution of a complex SAF candidate (left) and SPE extract of the same fuel (right)

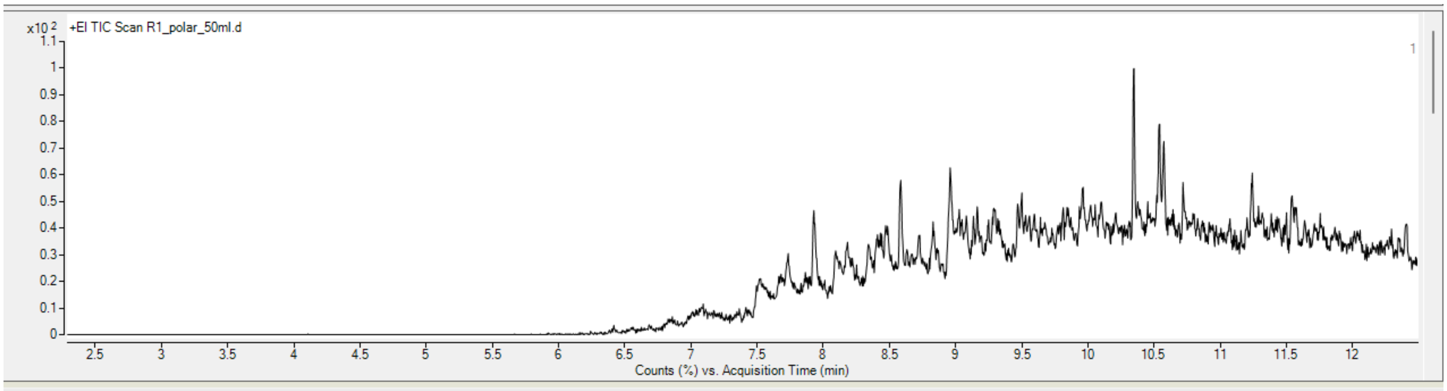

Figure 11. GC-MS chromatogram from conventional Jet A SPE extract.

Milestone

Isolated the polar fraction of real fuel samples from hydrocarbon matrix sufficiently well to identify several individual species.

Major Accomplishments

None.

Publications

None.

Outreach Efforts

None.

Awards

Conor Faulhaber, Distinguished Graduate Research Program (DGRP) appointment, Pacific Northwest National Laboratory (PNNL).

Student Involvement

Conor Faulhaber, a graduate student at WSU, worked with Research Faculty Zhibin Yang to develop this method capability, and leads its application towards the thermal stability project.

Plans for Next Period

- Improve GC-MS analysis for better identification of extracted polars.
- Scale-up the SPE method to larger volume suitable for doping studies.

References

Link, D. D., Baltrus, J. P., & Zandhuis, P., Hreha, D. C. (2005). Extraction, separation, and identification of polar oxygen species in jet fuel. *Energy and Fuels, 19*(4), 1693–1698. https://doi.org/10.1021/ef040095g

Link, D. D., Baltrus, J. P., & Zandhuis, P. (2007). Isolation and identification of nitrogen species in jet fuel and diesel fuel. *Energy & Fuels, 21*(3), 1575–1581. https://doi.org/10.1021/ef060451q

Yang, Z., Faulhaber, C., Boehm, R., Heyne, J. (2025). Geometric and Positional Isomer Effects on Ignition Behavior of Cycloalkanes: Implications for Sustainable Aviation Fuels. *Energy & Fuels, 39*(38), 18641–18648. https://doi.org/10.1021/acs.energyfuels.5c03856

Task 4 – Establish a Detailed Experimental Test Plan to Evaluate Thermal Stability

Washington State University

Objective

The objective of Task 4 is to outline in detail the approach to the thermal stability test campaign, including a description of how the required fuel volumes will be procured. The purpose of this test campaign is to evaluate the impact of natural polars from conventional fuel and PNNL's hydrothermal liquefaction (HtL) SAF candidate on thermal stability. Thermal stability will be measured using the JFTOT method outlined in Task 1.

Research Approach

The test plan is broken into two parts: baseline tests and design of experiment (DoE). The purpose of the baseline tests is to establish the thermal stability of the primary test fuels, a conventional Jet A fuel and a 10%v blend of HtL in the same Jet A fuel. HtL blending component volume limitations are the primary constraint in this test plan. While it is desirable to perform JFTOT testing on neat HtL, it is unlikely WSU SAF Lab will receive sufficient sample. On that note, it is worthwhile to mention that each JFTOT test requires approximately 600mL of fuel sample to be completed, and two to three replicates are desired due to the repeatability of the measurements, as shown in Task 1.

The test plan outlines the levels of impurities to be doped into each fuel, the nature of these dopants (nitrogen/sulfur levels, fuel source, etc.), and the temperatures to perform testing. The goal in this portion of the experimental design is to perform duplicate measurements at each level of JFTOT testing, while having spare fuel to test a third replicate if large variation is observed for a set of duplicates. The details of this test planned are outlined in Table 4.

Table 4. Thermal stability test campaign design of experiment.

Fuel	JFTOT Temperature [˚C]	Dopant from polar extract of Jet A	Dopant from cocktail simulating polar extract of HtL	Number of Replicates	HtL SBC Volume [L]
Baseline Tests					
Conventional Jet A	TBD (higher value)[1]	n/a	n/a	3	0
	TBD (lower value)[2]	n/a	n/a	3	0
HtL SAF/Jet-A 10/90 blend	Lower value	n/a	n/a	2	0.12
	Higher value	n/a	n/a	2	0.12
Impurity Concentration Derivatives					
HtL SAF/Jet-A 10/90 blend	TBD (lower value)[1]	High	High	2	0.12
	Lower value	Low	High	2	0.12
	Lower value	High	Low	2	0.12
	Higher value	High	High	2	0.12
	Higher value	Low	High	2	0.12
	Higher value	High	Low	2	0.12

[1] The higher test temperature shall not exceed the breakpoint of the petroleum fuel by more than 10 C and shall be at least as high as its breakpoint temperature. This set of tests shall be done first

[2] The lower test temperature shall produce at least one localized tube deposit of at least 60 nm when the most contaminated sample is tested but not more than 30 nm when the petroleum jet fuel sample is tested. In doing these trial-and-error experiments, a surrogate will be used to represent every aspect of the HtL to preserve HtL volume for the derivative study. The maximum levels of dopant concentration may be adjusted to ensure the lower test temperature satisfies both criteria.

JFTOT: jet fuel oxidation tester; HtL: hydrothermal liquefaction; SAF: sustainable aviation fuel; SBC: synthetic blend components; TBD: to be determined

Several levels of the test plan, including temperature, dopant composition, and dopant concentration, are still to be finalized. The footnotes on Table 4 address the upper and lower test temperatures. In order to get meaningful results, it is desired for the baseline Jet A fuel test at the higher temperature to reside near the Jet A fuel breakpoint. If temperature is too high the reaction could be driven to completion too quickly, meaning the deposition thickness could be driven more by dissolved oxygen concentration and/or deposit oxygen concentration than fuel quality. If lower test temperature is too low, then it will not be possible to measure the impact of fuel quality diversity. While the preliminary trial-and-error runs that are necessary to establish the upper and lower test temperature will require some reference petroleum jet fuel and some amount of a surrogate that represents the HtL synthetic blend components (SBC), neither of these materials are volume-limited within the context of this test matrix.

Dopant composition will be determined by the impurity amplification and characterization efforts outlined in Tasks 2 and 3. It is expected that the HtL extraction will define a dopant that is high in nitrogen. To preserve HtL volume for JFTOT testing, a surrogate (cocktail) that represents its polar extract will be created based on a recipe made from GC-MS characterization of the actual polar extract. The polar extract of the petroleum Jet A fuel is expected to be relatively high in sulfur content. Since we are not limited by the available volume of our reference petroleum fuel, its polar extracts can be collected until we have enough volume to satisfy the demand of the test plan. Testing these dopants at elevated levels in varying ratios in the HtL-Jet A blend will provide insight towards the impact of interactions between these two types of impurities on thermal stability, building on previous research (Zabarnick et al., 2019).

The two levels of dopant concentration shall be approximately one times (low) or three times (high) that of the blending component with which it is associated. For example, the low dopant level for the polars of the reference petroleum fuel will be created by extracting 540 ml of reference jet fuel, which would then be used to spike an untreated aliquot of 540 ml of the reference fuel. To complete a single test point with high dopant from the reference petroleum fuel will require approximately 2,160 ml of petroleum fuel (540 for the sample) and 60 ml of HtL SBC.

Fuel Procurement

HtL samples for this test plan will be procured from the PNNL team led by Huamin Wang. Conventional Jet A fuel will be procured from a local airport.

Milestones

- Completed the thermal stability test campaign design of experiment as outlined in Table 4 above.
- Developed contingency plans should the proposed plan run into further sample volume limitations.

Major Accomplishments

None.

Publications

None.

Outreach Efforts

Collaboration with the PNNL HtL team for procurement of their HtL SAF.

Awards

None.

Student Involvement

Conor Faulhaber, a graduate student at WSU, leads the HtL characterization effort within the WSU SAF Lab and acts as a liaison between PNNL and WSU on this project. He also is responsible for sourcing the Jet A from the local airport for this work, and aids in reporting on this task.

Plans for Next Period

Determine the exact temperature and doping levels for this task prior to executing the test plan. This will finalize the work for this task.

References

Zabarnick, S., West, Z. J., Schafer, L. M., Mueller, S. S., Striebich, R. C. (2019). Studies of the Role of Heteroatomic Species in Jet Fuel Thermal Stability: Model Fuel Mixtures and Real Fuels. *Energy & Fuels, 33*, 8557–8565. https://doi.org/10.1021/acs.energyfuels.9b02345

Task 5 – Execute Thermal Stability Test Campaign

Washington State University

Objective

The objective of Task 5 is to execute the test campaign outlined in Task 4 and provide full analysis of the results.

Research Approach

This test campaign will begin as soon as Tasks 1, 2, 3, and 4 are complete. Each of the first three tasks have proven to be more time consuming than originally envisioned, but we are now confident that they will be done within 6 months. From Task 1, the repeated asymmetrical streaking occurrence took a significant amount of time and resources to investigate, troubleshoot, and document to a point where the team felt comfortable moving forward with further JFTOT testing despite the occurrence of the streaking. During Task 2, the use of multiple sulfur methods to investigate low-sulfur detection required training and work on two additional, more complicated instruments than the UVF method and necessitated that the methods remain consistent with each other. Using the CIC method to probe the true LOD and LOQ of the UVF method made all three method development efforts interdependent. The GC-NCD also went through several different hardware configurations before its final state, requiring significant time for planning and site visits from technicians on top of method development. Task 3 and 4 both went roughly as planned, but Task 3 saw small challenges in the development of GC-MS techniques to characterize the amplified polars. A small obstacle with Task 4 was reassessing the amount of fuel that the PNNL HtL team would be able to provide.

Milestones

None.

Major Accomplishments

None.

Publications

None.

Outreach Efforts

None.

Awards

None.

Student Involvement

Conor Faulhaber, a graduate student at WSU, is responsible for leading the lab work associated with executing this experimental campaign. He is assisted by Kaamel Sidiqi, an undergraduate at WSU.

Plans for Next Period

Follow through on completing Task 5.

References

Not applicable.